**SERBIAN JOURNAL OF ELECTRICAL ENGINEERING**
**Vol. 23, No. 3, October 2026, 507-521**
**UDC: 621.391.812** **DOI: https://doi.org/10.2298/SJEE2603507E**
*Original scientific paper*

# Effects of Rain Attenuation in 6G Communication

**Sharmini Enoch[1], Ifiok Otung[2]**

**Abstract:** In 6G communication the use of higher frequencies above 7 GHz to up to 10 THz is considered. Above the 10 GHz frequency range the atmospheric propagation effects such as rainfall can produce considerable attenuation in the received signal. The aim of this work is to demonstrate the effects of rain attenuation in high frequencies. The radar rain data from Chilbolton Facility for Atmospheric and Radio Research (CFARR) facility at Chilbolton, UK is utilized to analyze the magnitude of attenuation caused by rain attenuation. The results indicate that at an operating frequency of 56.5 GHz, the predicted specific rain attenuation leads to a total path attenuation of approximately 48 dB for 0.01% of the annual time. This exceedance probability corresponds to high-intensity rainfall events and represents a critical availability threshold for millimeter-wave communication systems. Due to the short wavelength at 56.5 GHz, electromagnetic wave propagation is highly susceptible to scattering and absorption by raindrops, resulting in pronounced signal degradation.

**Keywords:** 6G, Rain attenuation, Radar, Chilbolton Facility, ITU-R Model.

## 1 Introduction

The aim of 6G communication is to provide high speed, low-latency communication with a speed which is multiple times faster than the 5G technology. 6G will range over the world in due course, in all kinds of areas and climates. The need for universal coverage and high data rates will require highest precision. Important applications include Internet of Things (IoT), medical instruments, autonomous vehicle communication, and areas in which precision is of overreaching importance [1]. For achieving a data rate of Tbps, 6G must acquire more bandwidth and other demanding performance. Utilizing the massively abundant spectrum over 100 GHz, including the THz band covering 0.1~10 THz and the optical band is the only solution. Compared to low-frequency

[1]Zayed University, College of Interdisciplinary studies, Dubai, UAE
sharmini.enoch@zu.ac.ae, https://orcid.org/0000-0002-3267-1066
[2]University of Bradford, UK, Faculty of Engineering and Informatics, Bradford, West Yorkshire, UK
i.otung@bradford.ac.uk, https://orcid.org/0000-0003-1442-3816

Colour versions of the one or more of the figures in this paper are available online at https://sjee.ftn.kg.ac.rs

© *Creative Common License CC BY-NC-ND*

bands, THz signal transmission suffers from some impairments. High path loss, gaseous attenuation, weather effects such as rain, snow, fog etc. absorb or scatter the incident signals since their physical dimensions are in the same order as the THz wavelength [2].

As frequency increases from the millimetre wave band to the THz band, the corresponding wavelength decreases. At these shorter wavelengths, atmospheric gaseous particles exhibit resonant behaviour, leading to higher attenuation compared to millimetre wave frequencies. Under rainy conditions, increased scattering and absorption at higher frequencies further enhance electromagnetic wave attenuation, as the distribution density of rain particles varies with wavelength. In addition, snow, cloud, and sleet particles possess distinct particle densities, which also contribute to signal attenuation. Atmospheric attenuation leads to power loss, resulting in a reduction of the received signal amplitude [3]. Frequency bands above 5 GHz experience higher signal loss during rainfall compared to lower-frequency bands. Rain-induced scattering distorts the signal and creates multipath propagation, which reduces the signal-to-noise ratio (SNR) and degrades overall data transmission quality [4]. Accurate channel modelling and characterization are crucial because high-frequency signals are extremely sensitive to atmospheric and environmental attenuation [5]. Rain attenuation can cause reduction in coverage range, decrease in throughput, and degraded quality of service for 6G networks [6].

In this work, the effects of rain attenuation and other atmospheric effects in high frequency communication is analysed. For microwave-band frequencies below approximately 50 GHz, there is an increase in the attenuation due to rain which is in proportion to the frequency. Around 100 GHz, there is a peak, above which the degree of attenuation remains steady or decreases. There is an increase in rain-induced attenuation which is in proportion to the rainfall intensity [7].

This paper is organised such that Section 2 presents the effects of rain attenuation. The experimental set up and measurements carried out in CFARR is illustrated in Section 3. The rain attenuation computation is presented in Section 4. The Cumulative distribution of rain attenuation is provided in Section 5. Section 6 gives the conclusion.

## 2 Effects of Rain Attenuation

Mainly based on experimental data, several empirical and semi-empirical rain attenuation prediction methods have been proposed over the years. The widely used predicting models currently are the ITU-R model and the Crane model [8]. The ITU-R.838-3 predicts the effect of rain attenuation in the terrestrial link. The rain attenuation increases with the length of the radio link and depends on the rainfall climatic conditions in the region where the link has to be installed for a given frequency and polarization [9].

## 2.1 Characterization of rain

Rain rate is a measure of the intensity of rainfall by calculating the amount of rain that exists over a given interval of time, provided the rainfall intensity is constant over that time period. The rain rate is expressed in terms of depth per unit time, for example mm/hr or inches/hr.

The stratiform rain is normally associated with the absence of strong up-draft of wind as well as large spatial coverage. It is mainly observed in the presence of melting layer; the temporal extent of this type of rain is normally few hours with relatively low rain fall rate (< 10 mm/hr). On the contrary, convective rain is associated with heavy rain fall, shorter time duration, strong wind up-draft and is a much more localized phenomenon. Due to this strong wind motion, melting layer is not normally observed in this case. Thus the melting layer is a good indicator for rain classification study [10].

Figs. 1 and 2 show the rain rate time series for the receiver site, which is to exemplify the nature of rain. These figures show the characterization of rain as stratiform and convective. During stratiform rain, the rain events produce a rain rate which is less than 10 mm/hr, the temporal extent of the rain is normally few hours in durations, and it extends to large spatial coverage. When convective events occur, there will be heavy rainfall, with shorter duration and with strong wind uplift [10]. These figures depict that the rain rate for both stratiform and convective rain events are quite significant and can affect the 6G signal attenuation.

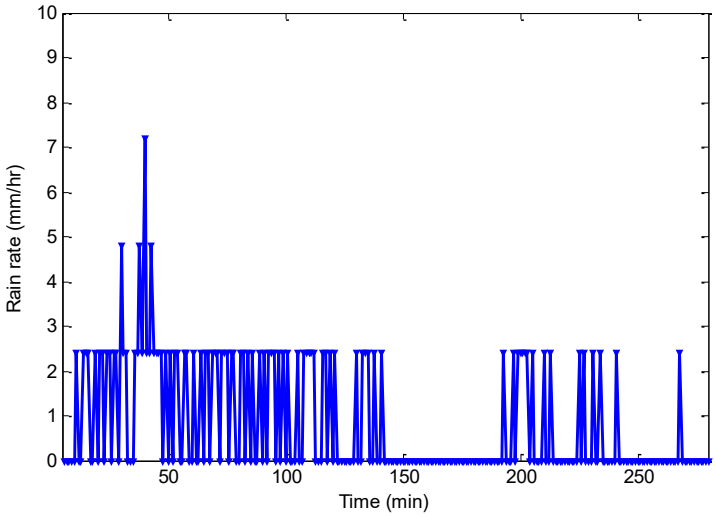



**Fig. 1** – *Rain rate time series showing stratiform events* (*rain rate* < 10 mm/hr).

The estimation of the long-term statistics of rain attenuation is performed by obtaining the rain rate $R_{0.01}$ exceeded for 0.01% of the time (with an integration time of 1 min) that is obtained from the information given in ITU-R.837-7 [11]. A time percentage of 0.01% of a year makes up to 53 minutes. Using ITU-R.838- 3, the specific attenuation $\gamma_R(p)$ (dB/km) for the frequency, polarization and rain rate are computed [12].

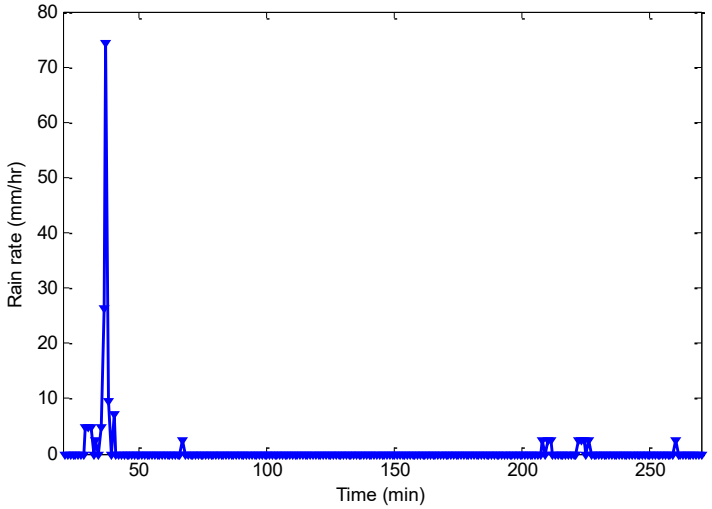



**Fig. 2** – *Rain rate time series showing convective rain event with rain rate in excess of* 70 mm/hr.

It is the fundamental quantity in calculating the rain attenuation. Its power-law form is written as:

$$\gamma_R(p) = kR^{\alpha}, \tag{1}$$

where $R$ is the rain rate in mm/hr, $k$ and α are the power law parameters, which depend on frequency, rain drop size distribution, rain temperature and polarization [13].

The rain attenuation exceeded during 0.01% of the time is given by ITU-R model as [14]:

$$\mathrm{A_p}\,(\mathrm{dB}) = \gamma_R(p)\, d_{\mathrm{eff}}(p), \tag{2}$$

where effective path length in km is given by:

$$d_{eff}(p) = dr, \tag{3}$$

where $d$ is the actual path length and $r$ is the distance factor,

$$r = \frac{1}{1+(d/d_0)} \tag{4}$$

and

$$d_0 = 35\mathrm{e}^{-0.015R_{0.01}}. \tag{5}$$

The estimation of the long-term statistics of rain attenuation is performed as illustrated in Fig. 3. It demonstrates the total rain attenuation for 2 km and 5 km path lengths. It can be observed that the total rain attenuation increases with increasing frequency and the overall attenuation is higher using horizontal polarization compared to vertical polarization. The higher rain attenuation observed for horizontal polarization is primarily attributed to the non-spherical shape of raindrops and their interaction with the electromagnetic field. As raindrops fall, aerodynamic forces cause them to assume an oblate (flattened) shape, with a larger horizontal than vertical axis. A horizontally polarized wave has its electric field aligned with this larger dimension, resulting in a greater effective interaction cross-section between the wave and the raindrop. This enhances both absorption and scattering losses compared to vertical polarization, whose electric field aligns with the smaller vertical axis of the drop. Consequently, the specific attenuation coefficient for horizontal polarization is higher than that for vertical polarization at the same frequency and rain rate, leading to increased overall attenuation in terrestrial microwave and millimetre-wave links.

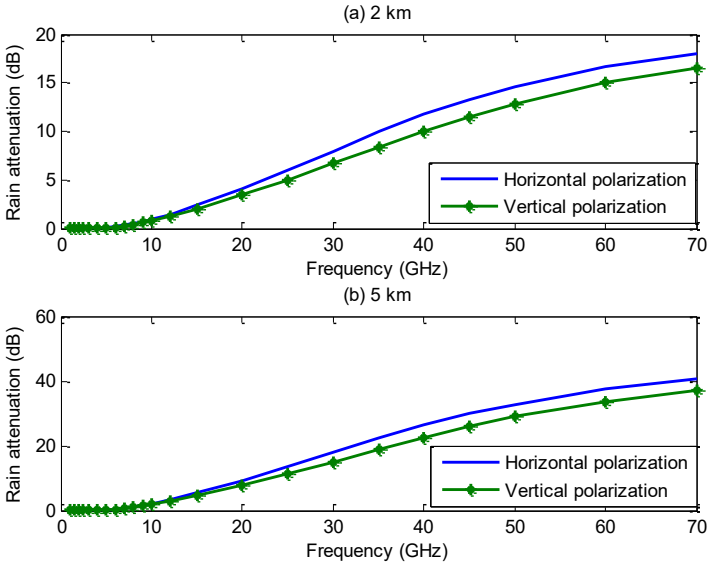



**Fig. 3** – *Rain attenuation from ITU-R model.*

## 3 Experimental Setup and Measurements using CFARR Facility

The experiments were conducted at the Chilbolton Facility for Atmospheric and Radio Research (CFARR) facility at Chilbolton, UK. The CFARR, located in the village of Chilbolton near Winchester in Hampshire (Latitude: 51.1445°N; longitude: 1.4370°W), has a ground-based atmospheric remote sensing facility. The CAMRa radar was used for the operation with the transmitter located at South Wonston (grid reference: SU 459 356; latitude: 51.117°N; longitude: 1.345°W; mean height above sea level: 120 m; height above ground: 27 m) and receiver at 5 km away at Sparsholt (grid reference: SU 425 320; latitude: 51.085°N; longitude: 1.394°W; mean height above sea level: 115 m; height above ground: 7 m; Receiver bearing from transmitter: 223°).

The CAMRa (Chilbolton Advanced Meteorological Radar) is a high-resolution, ground-based atmospheric radar capable of observing precipitation structure with fine spatial and temporal resolution.

From the radar, the following data products were used:

– Radar reflectivity ($Z$) along and around the radio link path
– Time-resolved precipitation observations**,** synchronized with RF measurements
– Spatial rainfall distribution**,** rather than single-point measurements.

The primary purposes of incorporating radar data were to:

– Identify precipitation events along the radio propagation path
– Quantify rainfall intensity responsible for attenuation
– Correlate signal fading with meteorological conditions
– Distinguish rain-induced attenuation from other effects (e.g., gaseous absorption, scintillation)
– Provide spatial and temporal context unavailable from point rain gauges alone

At 38 GHz, and above, rain is the dominant propagation impairment**,** making radar-derived rain information essential for causal attribution. This enabled rainfall to be analyzed over the entire 5 km propagation path, which is critical for short terrestrial links.

Radar reflectivity measurements were converted into rain rate ($R$, mm/hr) using standard empirical relationships of the form:

$$Z = \mathrm{a}\, R^{\mathrm{b}}, \tag{6}$$

where $Z$ is the radar reflectivity factor, $R$ is the rain and a and b is the empirically derived constants.

This conversion allowed radar data to be directly compared with measured signal attenuation**,** which depends on rain rate according to ITU-R propagation theory.

The aim of this link was to obtain a fixed terrestrial system operating at short range, low power, and LOS. The transmitter was erected on the tower platform 27 m above the ground, with the receivers erected on the Sparsholt cabin roof, 7 m above the ground forming the terrestrial radio. Locally gathered meteorological data and received signal strength from these links were simultaneously and continuously logged. The measurements were carried out over a four-year period from 2002 to 2005. Three continuous wave (unmodulated) linearly polarised signal transmissions at 38 GHz, 54.5 GHz and 56.5 GHz were supported by the 5 km link.

Figs. 4 and 5 show the terrain height of the LOS link. The three basic factors: earth curvature, Fresnel zone clearance ($K = 1.33$), and trees and growth are added for the obstacles that occur along the path [15]. In Fig. 5, the points A, B, C, and D mark the corrected obstacle points. It can be observed that the line joining the transmitter and receiver is clear of the obstacles after adding the correction factors.

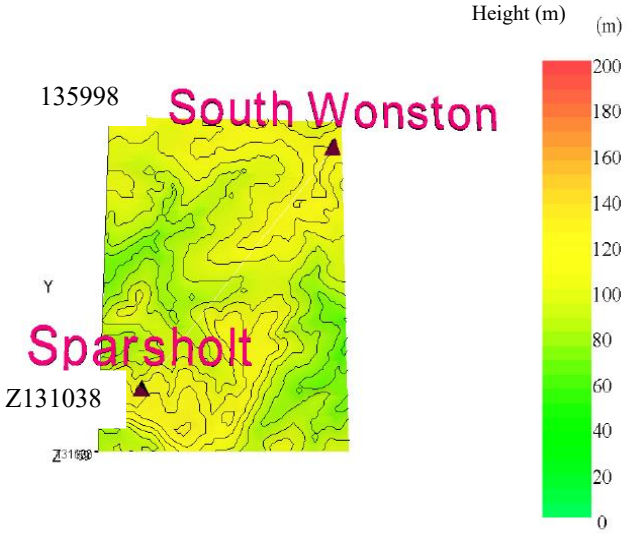



**Fig. 4 –** *Terrain height of transmitter and receiver location* [16].

The RF specifications are given in **Table 1**. The relative position of the link to the Chilbolton observatory is shown in Fig. 6.

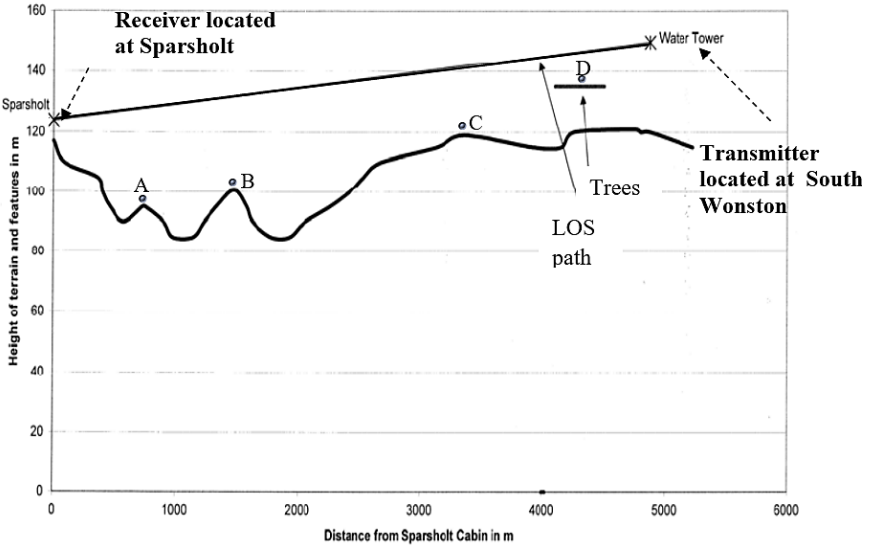



**Fig. 5** – *Land terrain for transmitter and receiver location* (*Adapted from* [17]).

**Table 1**

*RF unit specifications for transmitter and receiver* [17].

| R.F. Unit Specifications | Applies to both transmitter and receiver |
|---|---|
| Antenna type | Flann 2288TXCG-AD, 300 mm diameter high performance horn lens antenna to MPT1414 |
| Frequency range | 37.5 GHz to 39.5 GHz |
| Gain | 40 dBi |
| Beamwidth (half power) | 1.6° (E), 1.8° (H) |
| Waveguide | WG22 / R320 / WR28 |
| **Transmitter** | |
| Transmitter power | +15 dBm |
| Frequency range | 37.5 GHz to 39.5 GHz |
| Frequency stability | +/-2.5 ppm |
| Modulation type | 2 – level FSK |
| **Receiver** | |
| Double conversion | First I.F. =1220 MHz, Second I.F. =140 MHz |
| I.F. filter centred on 140 MHz | 6, 8 or 12 MHz depending on data rate |
| Threshold at $10^{-6}$ BER | -78 dBm |
| AGC output voltage range (with antennas removed as for back-to-back system calibration | Receiver input = -12.6 dBm, AGC = +4.04V d.c. Receiver input = -102.6 dBm, AGC = +0.47V d.c. |
| Receiver input for clear air level = -40.8 dBm, AGC = +2.58 V d.c. | |

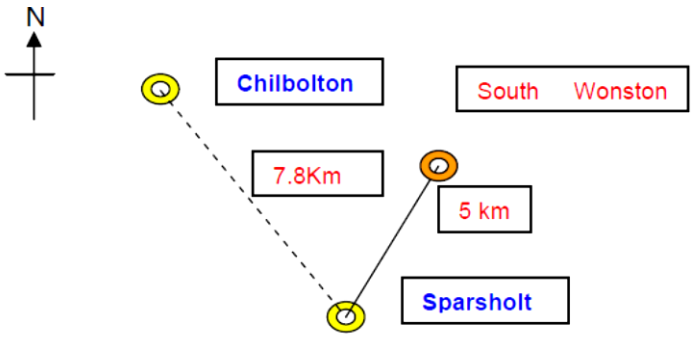



**Fig. 6** – *Relative position of the link to the Chilbolton Observatory* [7]. *Chilbolton Advanced Meteorological Radar (CAMRa).*

CAMRa is pulse radar installed at Chilbolton, South England. The radar is an active sensor that works by emitting a signal of given strength and measuring the amount of power reflected back by the hydrometeors in lower atmosphere [18]. The CAMRa radar is mounted on a 25 m diameter dish. Owing to the orientation of the 5 km link, the observations are possible to provide scans made along this path.

The characteristics of the radar are the following:

– Radar operating frequency: 3076.5 MHz

– Pulse repetition frequency: 610 Hz

– Pulse width: 0.5 μs

– Range resolution: 75 m

– Maximum number of range gates: 1200

– Maximum unambiguous range: 246 km

– Maximum unambiguous Doppler velocity: ±15 m/s.

## 4 Rain attenuation Computation

The data is in the NetCDF format. The information recorded in the data is shown in **Table 2**. The received power was measured for every 1 s sampling time. In a single day 86,399 samples were recorded. The overall rain attenuation is calculated from the power level as follows:

$$\text{Rain attenuation (dB)} = \text{Reference receiver power} - \text{Receiver power}, \quad (7)$$

where reference receiver power is the receiver power without clear-air effects and rain scatter, and receiver power is the power at receiver relative to the transmitter with all the units in dB.

**Table 2**
*NetCDF data information.*

| | |
|---|---|
| Link Identification | SouthWonston38 |
| Frequency | 38.79 GHz |
| Polarisation of transmit | Vertical |
| Polarisation of receive | Vertical |
| Latitude transmitter | 51.117°N |
| Longitude transmitter | 1.345°W |
| Latitude receiver | 51.085°N |
| Longitude receiver | 1.394°W |
| National grid reference transmitter | SU 459 356 |
| National grid reference receiver | SU 427 318 |
| Transmitter altitude AMSL | 120 m |
| Receiver altitude AMSL | 115 m |
| Link length | 5 km |
| Reference receiver power | - 41.5 dBm |
| Time | 86,399 samples per day |
| Receiver power | 86,399 samples per day |

Fig. 7 shows the histogram of rainy hours classified according to rain intensity derived from meteorological radar data. Each bar shows how frequently each rain type occurred**,** based on radar-derived rain rates. The results indicate that light and moderate rainfall events dominate in occurrence, while heavy and very heavy rain events occur less frequently but contribute significantly to high attenuation levels at millimetre-wave frequencies. **Table 3** provides the classification of rain type based on the rain rate.

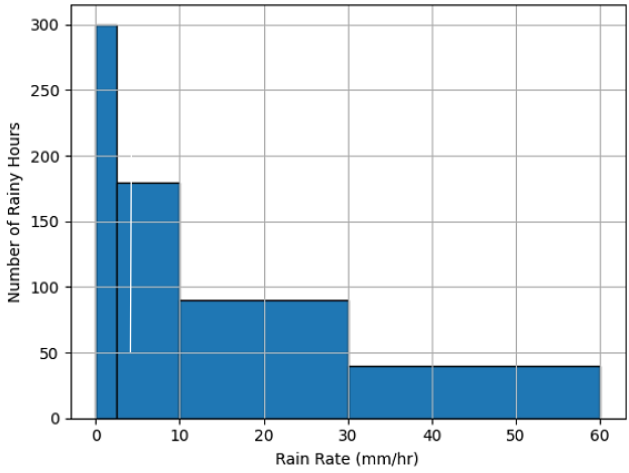



**Fig. 7** – *Histogram of Number of rainy hours versus Rain rate.*

**Table 3**
*Rain Classification.*

| Rain type | Rain rate (mm/hr) |
|---|---|
| Light rain | 0.1 – 2.5 |
| Moderate rain | 2.5 – 10 |
| Heavy rain | 10 – 30 |
| Very heavy rain | > 30 |

Fig. 8 illustrates the attenuation time series for a single day. The maximum fade level reaches up to 15.8 dB for that day. The deep fades obtained are observed only during certain time samples, but this level significantly varies while considering the data for a full year.

In order to observe the loss pattern for the year, Cumulative Distribution Function (CDF) plots are essential. The quality check of the attenuation time series $A_p$ (dB) is done by comparing its CDF with the CDF predicted using the ITU-R model and the statistical rain rate at 0.01% ($R_{0.01}$ mm/h) for the reference location.

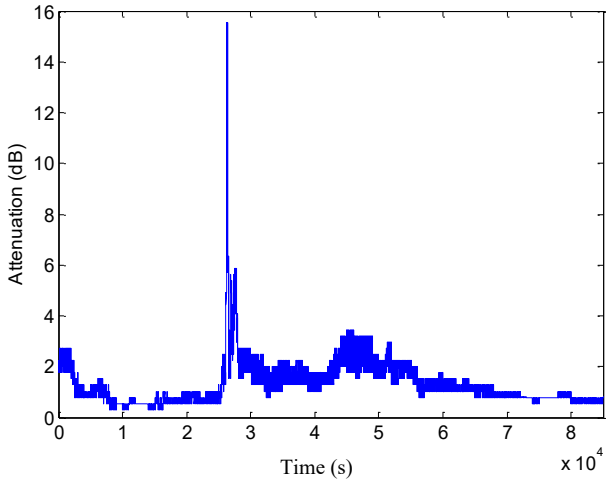



**Fig. 8 –** *Attenuation time series on* 16-7-2003 *at* 38 GHz.

## 5 Cumulative Distribution of Rain Attenuation

The Cumulative distribution of the rain attenuation that is calculated in the previous section is plotted in Figs. 9 to 11 for various frequencies. It demonstrates the annual cumulative distribution from 2003 to 2005 is compared with the ITU- R model. The data provides agreement at certain percentages of time. The

results in Fig. 9 demonstrate that for 38 GHz frequency (data from 2003) for 0.01% of time an attenuation of 40 dB is obtained. The results in Fig. 10 illustrates that at 54.5 GHz frequency (data from 2004), for 0.01% of time an attenuation of 46 dB is obtained. At 56.5 GHz frequency (data from 2005), an attenuation of about 48 dB is obtained for 0.01% of time as in Fig. 11.

**Table 4** depicts the rain attenuation for 0.01% of time for various frequencies comparing the experimental data with ITU-R model. All the results demonstrate that rain attenuation can cause significant signal losses at higher frequencies that are utilized in the 6G networks

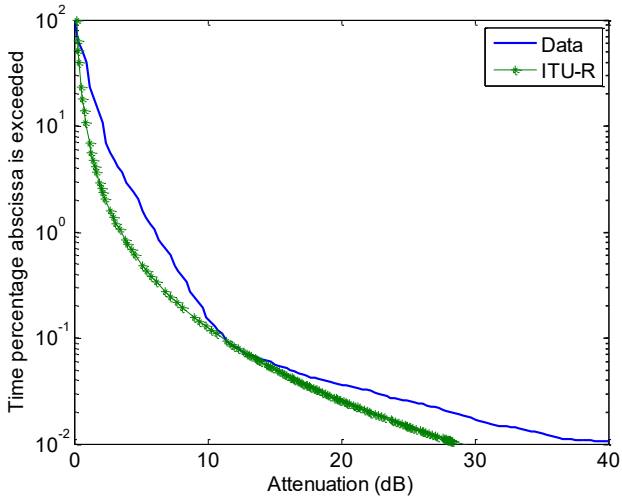



**Fig. 9 –** *Cumulative distribution of observed rain attenuation for a year of data at* 38 GHz (2003) *compared with ITU-R predictions.*

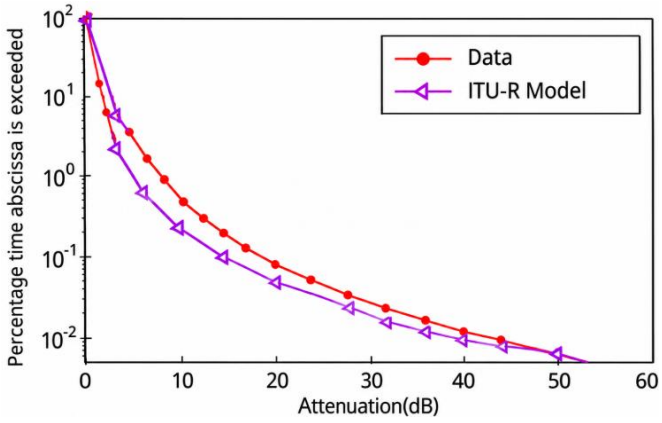



**Fig. 10. -** *Cumulative distribution of observed rain attenuation for a year of data at* 54.5 GHz (2004) *compared with ITU-R predictions.*

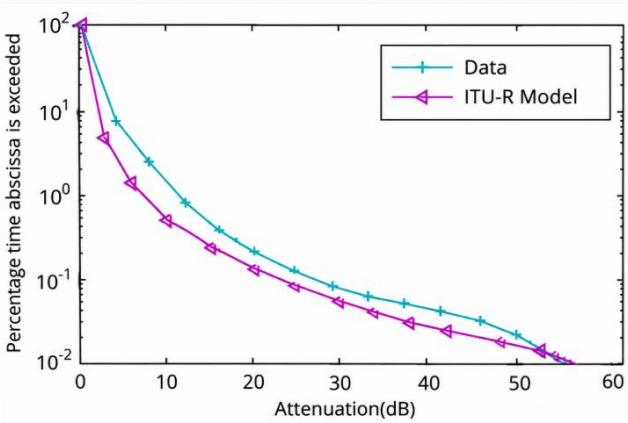



**Fig. 11 –** *Cumulative distribution of observed rain attenuation for a year of data at* 56.5 GHz (2005) *compared with ITU-R predictions.*

**Table 4**
*Time percentage of* 0.01% *values of Rain attenuation calculated by ITU-R predictions and Data.*

| Frequency | Rain attenuation $A_{0.01}$ (ITU-R) | Rain attenuation $A_{0.01}$ (Data) |
|---|---|---|
| 38 GHz | 28 dB | 40 dB |
| 54.5 GHz | 47 dB | 46 dB |
| 56.5 GHz | 47 dB | 48 dB |

### 5.1 Correlation between rain rate and signal attenuation

Fig. 12 shows the correlation between radar-derived rain rate and measured signal attenuation at 38 GHz. A strong positive correlation (Pearson $r \approx 0.98$) is observed, indicating that signal degradation increases significantly with increasing rainfall intensity. This confirms that rain attenuation is the primary cause of signal loss at this frequency, consistent with ITU-R propagation models.

## 6 Conclusion

High frequency communication such as 6G will enable plenty of applications. In 6G the effects of atmospheric impairments such as rain can significantly affect the signal quality due to attenuation. The Chilbolton 5 km propagation measurements have provided valuable insight into rain-induced attenuation at frequencies of 38 GHz and above. The results show that at 56.5 GHz, rain attenuation reaches as high as 48 dB for 0.01% of the time (approximately 53 minutes per year), demonstrating the severe vulnerability of V-band links to intense precipitation events. Even lower attenuation levels, such

as 11 dB at 0.01% time, can significantly degrade link performance by reducing carrier-to-noise ratio (C/N), increasing bit error rate (BER), and compromising quality of service (QoS) targets for high-capacity backhaul and emerging 6G systems. The close agreement between the measured cumulative attenuation distribution and the predictions of the International Telecommunication Union Radiocommunication (ITU-R) model validates the reliability of established propagation models for high-frequency terrestrial links. These findings confirm that accurate rain attenuation prediction is essential for robust link design, particularly in regions with high rainfall rates. To ensure stringent availability targets (e.g., 99.99%), system designers must incorporate adequate fade margins and advanced mitigation strategies such as adaptive modulation and coding (AMC), transmit power control, and diversity techniques. Overall, this study reinforces the critical importance of precise propagation modeling and adaptive system design in enabling reliable high-frequency communication networks.

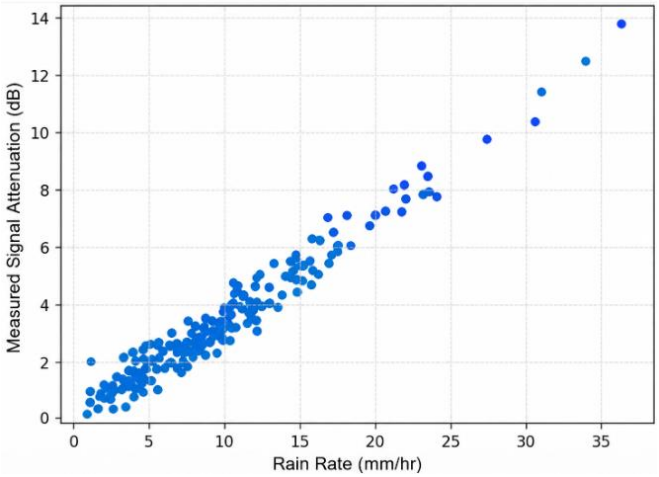



**Fig. 12. –** *Correlation between Rain rate and Signal Attenuation at* 38 GHz *Pearson r* = 0.98.

## 7 References

[1] J. Kupferman, S. Arnon: Communication Systems Performance at mm and THz as a Function of a Rain Rate Probability Density Function Model, Sensors, Vol. 22, No. 16, August 2022, p. 6269.

[2] W. Jiang, H. D. Schotten: Full-Spectrum Wireless Communications for 6G and Beyond: From Microwave, Millimeter-Wave, Terahertz to Lightwave, Proceedings of the IEEE 3rd International Conference on Computer Communication and Artificial Intelligence (CCAI), Taiyuan, China, May 2023, pp. 353 – 357.

[3] M. E. Shawon, M. Z. Chowdhury, M. B. Hossen, M. F. Ahmed, Y. Min Jang: Rain Attenuation Characterization for 6G Terahertz Wireless Communication, Proceedings of the

International Conference on Artificial Intelligence in Information and Communication (ICAIIC), Jeju Island, South Korea, April 2021, pp. 416 – 420.

[4] S. Goyal, R. K. Yadav: Impact of Rainfall on the Wireless Transmission of Signals, Proceedings of the 5th International Conference on Advancement in Electronics & Communication Engineering (AECE), Ghaziabad, India, November 2025, pp. 1191 – 1193.

[5] B. Khan, J. Kokkoniemi: Analysis of Path Losses on Terahertz Band for Non-Terrestrial Networks, IEEE Transactions on Vehicular Technology, Vol. 75, No. 7, July 2026, pp. 13643 – 13658.

[6] M. F. Abughalia, O. Boiprav, A. R. Zerek, S. E. A. Abeid: The Effect of Rain Attenuation on the Efficiency of Wireless Communication Systems in Millimeter Wave Frequencies, Proceedings of the IEEE 22nd International Conference on Sciences and Techniques of Automatic Control and Computer Engineering (STA), Hammamet, Tunisia, December 2025, pp. 741 – 746.

[7] S. Ishii, M. Kinugawa, S. Wakiyama, S. Sayama, T. Kamei: Rain Attenuation in the Microwave-to-Terahertz Waveband, Wireless Engineering and Technology, Vol. 7, No. 2, April 2016, pp. 59 – 66.

[8] N. A. Pérez García, L. A. R. da Silva Mello: Improved Method for Prediction of Rain Attenuation in Terrestrial Links, Electronics Letters, Vol. 40, No. 11, May 2004, pp. 683 – 684.

[9] F. Fedi: Prediction of Attenuation due to Rainfall on Terrestrial Links, Radio Science, Vol. 16, No. 5, September 1981, pp. 731 – 743.

[10] S. Das, A. K. Shukla, A. Maitra: Classification of Convective and Stratiform Types of Rain and their Characteristics Features at a Tropical Location, Proceedings of the 4th International Conference on Computers and Devices for Communication (CODEC), Kolkata, India, December 2009, pp. 1 – 4.

[11] Characteristics of Precipitation for Propagation Modelling, ITU-R P.837-8, 2025.

[12] Specific Attenuation Model for Rain for Use in Prediction Methods, ITU-R P.838-3, 2005.

[13] T. Mao, D. Zhou, Z. Niu: The Calculation Model of the Attenuation Due to Clouds and Fog and the Analysis of its Characteristic, Proceedings of the Asia-Pacific Radio Science Conference, Qingdao, China, August 2004, pp. 332 – 334.

[14] Propagation Data and Prediction Methods Required for the Design of Terrestrial Line-of-Sight Systems, ITU-R P.530-19, 2025.

[15] R. L. Freeman: Fundamental of Telecommunications, 2nd Edition, John Wiley & Sons, Inc., Hoboken, 2005.

[16] Science and Technology Facilities Council, Chilbolton Facility for Atmospheric and Radio Research, Natural Environment Research Council, C. L. Wrench: Chilbolton Facility for Atmospheric and Radio Research (CFARR) South Wonston to Sparsholt 5 km 38 GHz radio link data, NCAS British Atmospheric Data Centre, 2003, Available at: https://catalogue.ceda.ac.uk/uuid/85d0042eb287eacd497e48a0a99499fa

[17] South Wonston to Sparsholt 5 km radio links, Chilbolton Observatory, U.K, 2003, Available at: https://artefacts.ceda.ac.uk/badc_datadocs/chilbolton/links.html.

[18] A. Pawlina-Bonati: Essential Knowledge of Rain Structure for Radio Applications Based on Available Data and Models, Proceedings of the Third Regional Workshop on Radio Communication in Africa – Radio Africa, Gaborone, Botswana, October 1999, pp. 96 – 106.